

General Theory of Spontaneous Emission Near Exceptional Points

A. Pick,^{1,*} B. Zhen,^{2,*} O. D. Miller,³ C. W. Hsu,⁴ F. Hernandez,³
A. W. Rodriguez,⁵ M. Soljačić,² and S. G. Johnson^{2,3}

¹*Department of Physics, Harvard University, Cambridge, Massachusetts 02138, USA*

²*Department of Physics, Massachusetts Institute of Technology, Cambridge, Massachusetts 02139, USA*

³*Department of Mathematics, Massachusetts Institute of Technology, Cambridge, Massachusetts 02139, USA*

⁴*Department of Applied Physics, Yale University, New Haven, Connecticut 06520, USA*

⁵*Department of Electrical Engineering, Princeton University, Princeton, New Jersey 08544, USA*

Exceptional points (EPs)—non-Hermitian degeneracies where both the eigenvalues and the eigenvectors coalesce—have recently been realized in various optical systems. Here we present a general theory of spontaneous emission near such degeneracies, where standard mode-expansion methods lead to erroneous divergent results. We show that significant (and finite) enhancements for light-matter interaction can occur in systems with gain, whereas in passive systems the enhancement is at most four-fold. Under special conditions, the emission spectral lineshape near the EP becomes a squared Lorentzian, and the enhancement scales quadratically with the resonance lifetime.

While it is well known that electromagnetic resonances can enhance spontaneous emission (SE) rates via the Purcell effect [1–3] by confining light to small volumes for long times, recent work [4–6] suggests that giant enhancements can occur via the less familiar Petermann effect [7–11], caused by non-orthogonality of the modes in open resonators. The Petermann enhancement factor (PF) scales inversely with the unconjugated “inner product” of the resonant mode, and it appears to diverge when two modes merge into an *exceptional point* (EP)—a degenerate resonance where both the eigenvalues and the eigenvectors coalesce [12–14]. One might naively expect that SE diverges at the EP as well, or at least that peculiar emission properties arise. However, we show in this Letter that SE enhancement at the EP is finite—it stops growing once the resonance peaks overlap. The limit is given analytically in terms of the degenerate mode and an additional Jordan vector [13, 15, 16], generalizing earlier results limited to one dimension [17] and results derived for discrete oscillator systems [18], which lack an asymptotic formula. We show that significant enhancements can occur in systems with gain, whereas in passive systems the enhancement is at most four-fold. Moreover, under special conditions, the enhancement scales quadratically with the resonance lifetime. Our results provide a quantitative prescription for achieving large enhancements in practice, which can be implemented with the recent experimental realizations of EPs [19–23].

We begin by reviewing SE theory for non-degenerate resonances and proceed by presenting the corrected formulation at the EP. To illustrate our results, we employ a two-dimensional plasmonic system consisting of two coated metallic rods, with gain and loss in the coatings. Motivated by the fact that an EP is associated with a double pole in the Green’s function, we find specific locations where the emission lineshape becomes a squared Lorentzian, with peak amplitude scaling as $1/\gamma^2$, where γ

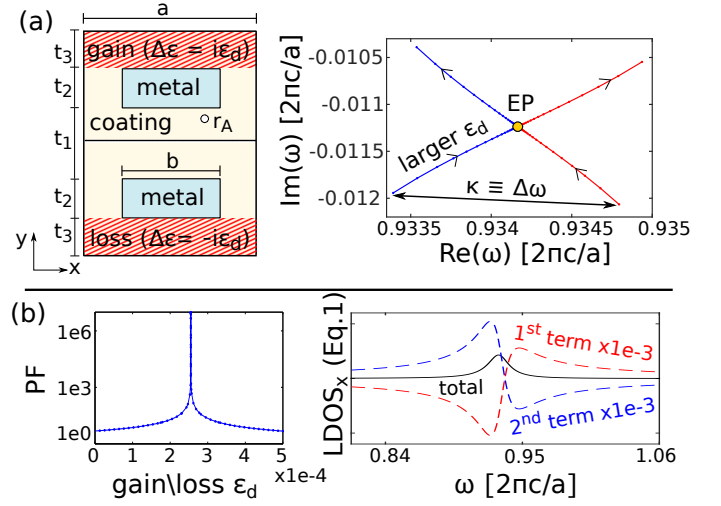


FIG. 1. **Infinite Petermann factor (PF) and finite LDOS at an EP.** (a) Left: Two plasmonic resonators with metallic cores and dielectric coatings. Gain and loss ($\pm i\epsilon_d$) are added to the outer sides of the coatings. Right: Eigenvalue trajectories in the complex plane for $\epsilon_d \in (0, 0.00045)$. An EP occurs at $\epsilon_d \approx 0.00025$. (b) Divergent PF $\equiv (E_n^{R*}, E_n^R)(E_n^{L*}, E_n^L) / |(E_n^L, E_n^R)|^2$ (left) and finite LDOS_x (right) at the EP. Individual terms in Eq. (1) (blue/red curves, scaled by 10^{-3}) blow up near the EP, while their sum (black) remains finite. [Eq. (1) is evaluated at \mathbf{r}_A , shown in (a).]

is the resonance decay rate. The enhancement at the EP is thus potentially much larger than the Purcell factor, which scales as $1/\gamma$. Then, we extend our formalism to periodic structures. Using a system that allows us to independently tune gain, loss, and degeneracy, we demonstrate that significant PF enhancements can be achieved with gain. Last, we derive a general upper bound on the enhancement at the EP for arbitrary low-loss systems.

The figure of merit for SE rates is the local density of states (LDOS) [24–26] which, semi-classically, is the power expended by a dipole source. The LDOS at frequency ω , polarization ℓ , and position \mathbf{r} is related to

* These authors contributed equally to this work.

the dyadic Green's function $G_{\mu\nu}$ via: $\text{LDOS}_\ell(\mathbf{r}, \omega) = -\frac{2\omega}{\pi} \text{Im}[G_{\ell\ell}(\mathbf{r}, \mathbf{r}, \omega)]$ [24, 27, 28]. Near structures with discrete non-degenerate resonances ($\omega_n = \Omega_n + i\gamma_n$), it is convenient to compute the Green's function with the standard modal expansion formula [29]. For systems with spectrally separated low-loss resonances, the LDOS is approximately a sum of Lorentzians [28]:

$$\text{LDOS}_\ell(\mathbf{r}, \omega) \approx \sum_n \frac{1}{\pi} \frac{\gamma_n}{(\omega - \Omega_n)^2 + \gamma_n^2} \text{Re} \left[\frac{E_{n\ell}^L(\mathbf{r}) E_{n\ell}^R(\mathbf{r})}{(E_n^L, E_n^R)} \right]. \quad (1)$$

This result is valid for systems with low losses. For arbitrary losses, there is an additional term in Eq. (1) $\propto \text{Im}[E_{n\ell}^L E_{n\ell}^R / (E_n^L, E_n^R)]$. Here, $E_{n\ell}^R$ is the ℓ th component of the vector \mathbf{E}_n^R , which is an outgoing solution of Maxwell's equations or, more explicitly, is a right eigenvector of the eigenvalue problem: $\hat{A} \mathbf{E}_n^R = \omega_n^2 \mathbf{E}_n^R$ [30], with $\hat{A} \equiv \varepsilon^{-1} \nabla \times \nabla \times$. Left modes (\mathbf{E}_n^L) are eigenvectors of the transposed operator $\hat{A}^T \equiv \nabla \times \nabla \times \varepsilon^{-1}$. Right and left modes which correspond to different eigenvalues are orthogonal under the unconjugated "inner product" $(E_n^L, E_m^R) \equiv \int d\mathbf{r} \mathbf{E}_n^L \cdot \mathbf{E}_m^R = \delta_{m,n}$ [31–33]. Consequently, in the limit where two modes coalesce at an EP, the degenerate mode is self-orthogonal [12], leading to divergence of individual terms in Eq. (1), as well as divergence of the PF $\equiv (E_n^{R*}, E_n^R)(E_n^{L*}, E_n^L) / |(E_n^L, E_n^R)|^2$ [5].

However, in reality, the LDOS remains finite at the EP even though the PF diverges. In the Supplemental Material (SM) we prove that the two terms Eq. (1) tend to infinity at the same rate and with opposite signs, so that their sum remains finite [Eq. (S14)]. The key to a quantitative understanding of LDOS at EPs is to recognize that the standard Green's function expansion formula [29] is inadequate because the set of eigenvectors at an EP does not span the Hilbert space. In order to complete the basis, one must use both the eigenvector \mathbf{E}_0^R and the Jordan vector \mathbf{J}_0^R , which satisfy the chain relations [13, 15, 16]

$$\begin{aligned} A_0 \mathbf{E}_0^R &= \omega_{\text{EP}}^2 \mathbf{E}_0^R \\ A_0 \mathbf{J}_0^R &= \omega_{\text{EP}}^2 \mathbf{J}_0^R + \mathbf{E}_0^R, \end{aligned} \quad (2)$$

with similar expressions for left eigenvectors. The mathematical procedure of Green's function expansion at EPs has been carried out previously [34–36], but was not applied to the LDOS, and in the SM we provide a condensed derivation of this result. The resulting expression is

$$G_{\text{EP}}(\mathbf{r}, \mathbf{r}', \omega) \approx \frac{\mathbf{E}_0^L(\mathbf{r}) \mathbf{E}_0^R(\mathbf{r}')}{(E_0^L, J_0^R)(\omega^2 - \omega_{\text{EP}}^2)^2} + \frac{\mathbf{E}_0^L(\mathbf{r}) \mathbf{J}_0^R(\mathbf{r}') + \mathbf{J}_0^L(\mathbf{r}) \mathbf{E}_0^R(\mathbf{r}')}{(E_0^L, J_0^R)(\omega^2 - \omega_{\text{EP}}^2)}, \quad (3)$$

where we have chosen $(J_0^L, J_0^R) = 0$ and $(E_0^L, J_0^R) = 1$. For low-loss systems, Eq. (3) implies that when the second term is small, the lineshape is a squared Lorentzian, with peak value scaling as $1/\gamma^2$, where $\gamma \equiv \text{Im}[\omega_{\text{EP}}]$.

We numerically demonstrate the implications of Eq. (3) for the plasmonic system of Fig. 1a, consisting of two rods with metallic cores ($\varepsilon = -2.3 + 0.0001i$) and silica coatings ($\varepsilon = 2.1316$) in air ($\varepsilon = 1$). Outgoing boundary conditions are implemented using perfectly matched

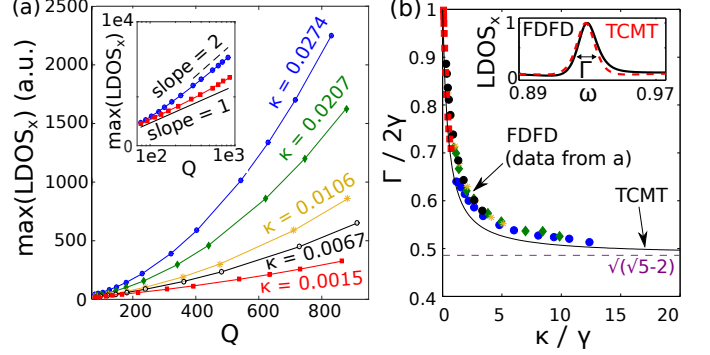


FIG. 2. **Quadratic scaling and spectral narrowing of the LDOS at EPs.** (a) LDOS peak vs. quality factor Q , showing quadratic (linear) scaling for large (small) coupling values κ . The LDOS_x is evaluated at \mathbf{r}_A for the structure from Fig. 1a using FDFD. Q is varied by adding gain to the coatings, while κ is varied by changing the rod-rod separation (t_1). Inset: Red and blue points from the main plot, on a log-log scale. (b) Normalized linewidth at the EP ($\Gamma/2\gamma$) vs. normalized coupling (κ/γ), computed using FDFD (symbols) and TCMT [Eq. (S29), black line]. The limit is shown in purple (dashed line). Inset: LDOS_x at the EP, computed via FDFD (black) and TCMT [Eq. (S28), red dashed line].

layers (PML) [28]. The dimensions of the structure are: $b = 0.643a$, $t_1 = 0.536a$, $t_2 = 0.16a$, and $t_3 = 0.268a$. Gain and loss are added symmetrically to the outer parts of the coatings. By brute-force optimization, we find that an EP occurs when $|\Delta\varepsilon| \approx 0.0002551$, and the background permittivity of the upper coating is $\text{Re} \varepsilon \approx 2.129$; the trajectories of the two complex eigenvalues near the EP are shown in Fig. 1a. We discretize Maxwell's equations using a finite-difference frequency-domain (FDFD) approach [37], and we compute the LDOS_x using three methods: (i) direct computation of the full Green's function, (ii) using Eq. (1) while including both modes near the EP, and (iii) using the limiting expression Eq. (3) at the EP. Near the EP, we find that all three methods agree, provided that the LDOS is dominated by the two coalescing modes. Fig. 1b shows the divergent PF and the finite LDOS at the EP that results from cancellation of the two diverging terms in Eq. (1).

It is useful to introduce a simplified model to interpret the results, which is valid when the rods are weakly coupled [i.e., when the rod-rod separation (t_1) is large enough so that the frequency splitting induced by the coupling (κ) is smaller than the uncoupled resonance frequencies]. The dynamics of the system can then be described by temporal coupled-mode theory (TCMT) [38]:

$$\dot{\mathbf{a}} = i \begin{pmatrix} \Omega_{\text{EP}} + i\gamma - i\eta & \kappa \\ \kappa & \Omega_{\text{EP}} + i\gamma + i\eta \end{pmatrix} \mathbf{a} \equiv i\mathbf{H}\mathbf{a} \quad (4)$$

(reviewed in the SM). Here, $\mathbf{a} = [a_1; a_2]$ are the mode amplitudes of the two uncoupled resonators, $\Omega_{\text{EP}} - i\gamma$ is the degenerate eigenvalue, and κ is the frequency splitting induced by the rod-rod coupling (Fig. 1a). In general,

a) Exceptional points in PhC waveguides

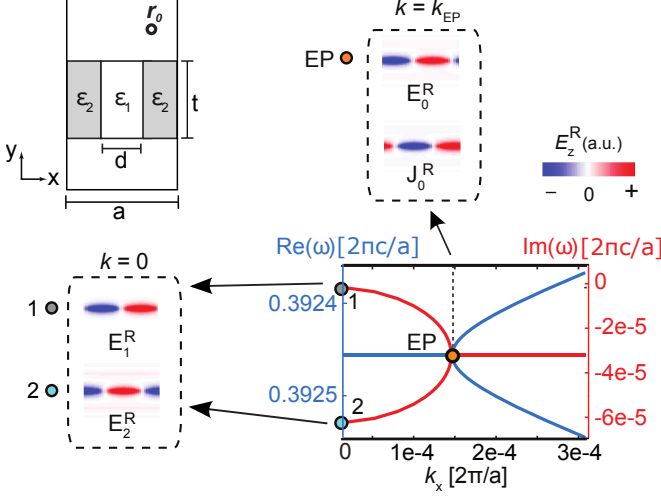


FIG. 3. (a) Top left: Periodic waveguide with outgoing boundary condition in the transverse direction. TM modes at $k = 0$ (bottom left) and the degenerate mode and Jordan vector at k_{EP} (top right). [Only $\text{Re}(E_z^R, J_z^R)$ are shown]. Bottom right: Complex resonances ω_n vs. k -vector, showing an EP at $k_{EP}a/2\pi \approx 1.46 \times 10^{-4}$. (b) Top-upper plot: LDOS $_k$ at $\mathbf{r} = \mathbf{r}_0$ for four k -values (k_{EP} , k_1 , k_2 , k_∞ , as marked on the lower plot). Top-lower plot: Resonances $\omega_n(k)$ in the complex plane. Bottom: Normalized LDOS $_k$ peak (M_k/M_∞) vs. deviation from the EP (Δk) for four Q values, showing 4-fold enhancement at the EP.

κ is complex but in this system, it is almost real and, for easy of discussion, we approximate it by $\text{Re} \kappa$. Last, $\eta \approx \frac{\Omega_{EP}}{2} \frac{\int E_n^L(\Delta\varepsilon/\varepsilon) E_{nx}^R}{(E_n^L | E_{nx}^R)}$ is the imaginary frequency shift induced by nonzero gain/loss ($\Delta\varepsilon$) in the coatings. (The integration in the numerator is over the upper coating. This result follows from perturbation theory for small gain/loss [30].) An EP occurs at $\eta = \kappa$.

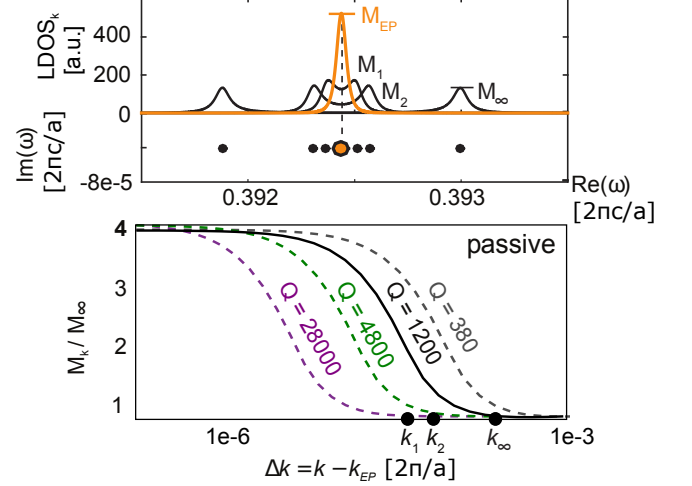
This simplified model produces an approximate formula for the LDOS at the EP [Eq. (S27) in SM], which is valid near the resonators. The approximate LDOS formula contains a term $\propto \kappa/\gamma^2$ and a term $\propto 1/\gamma$; the explicit lineshape, however, depends on the precise location where the LDOS is evaluated and on the realness of the modes. When the eigenmodes are almost real (which is valid for low-loss systems), the LDOS lineshape near the upper (low-loss) resonator is approximately a squared Lorentzian, with a peak value (M_{EP}) that scales as

$$M_{EP} \propto \frac{1}{\gamma} + \frac{\kappa}{\gamma^2}. \quad (5)$$

When the resonance-decay rate γ is much smaller than the mode-coupling rate κ , M_{EP} scales quadratically with the quality factor $Q \equiv \frac{\Omega_{EP}}{2\gamma}$ [30] [in contrast to isolated resonances, for which M_{EP} scales linearly with Q].

In Fig. 2a, we verified Eq. (5) by computing M_{EP} via FDFD for fixed rod-rod separations (i.e., fixed κ) while adding background gain to modify Q . We repeated this procedure for five couplings (κ), and observed the quadratic scaling at large couplings and high quality factors. Another implication of the squared-Lorentzian lineshape is a narrower emission peak, as shown in Fig. 2b. In the limit of $\kappa/\gamma \rightarrow \infty$, the full-width half maximum

b) Bounded enhancement for passive EPs



(FWHM) approaches $\sqrt{\sqrt{5} - 2} \approx 0.48$ times the FWHM of a non-degenerate resonance 2γ [details in the SM, Eq. (S29)]. The TCMT LDOS lineshape also agrees well with FDFD (inset of Fig. 2b).

Next, we extend our formalism to periodic structures [30], which offer a convenient way to tailor the LDOS in practice. The modes of a periodic system are of the form $\mathbf{E}(\mathbf{r}) = \mathbf{E}_k(\mathbf{r})e^{i\mathbf{k}\cdot\mathbf{r}}$, where $\mathbf{E}_k(\mathbf{r})$ is a periodic function and \mathbf{k} is the wavevector [39]. At each \mathbf{k} , the mode $\mathbf{E}_k(\mathbf{r})$ solves an eigenvalue problem of the form: $A(\mathbf{k})\mathbf{E}_{nk} = \omega_{nk}^2\mathbf{E}_{nk}$, where $A(\mathbf{k}) \equiv \varepsilon^{-1}(\nabla + i\mathbf{k}) \times (\nabla + i\mathbf{k}) \times$. The power expended by a Bloch-periodic source with a particular k -vector and polarization ℓ is the LDOS $_{\ell k}$, which we abbreviate as LDOS $_k$ (also called the mutual density of states [40]). Integrating the LDOS $_k$ over the Brillouin zone produces the LDOS.

Fig. 3a presents an example of a periodic structure which consists of a waveguide with periodic index modulation along its central axis (\hat{x}). PML is used to truncate the transverse (\hat{y}) direction. The design parameters are: $\varepsilon_1 = 12, \varepsilon_2 = 13.137, d = 0.49a$, and $t = 0.25a$. We force an EP for TM-polarized modes (E_z, H_x, H_y) by fine-tuning the wavevector k_x and the permittivity contrast $\Delta\varepsilon \equiv \varepsilon_2 - \varepsilon_1$ (see Fig. S1). At $\mathbf{k} = 0$ (also called the Γ point), Maxwell's eigenvalue problem is complex-symmetric and, consequently, the eigenvectors \mathbf{E}_1^R and \mathbf{E}_2^R are orthogonal (lower-left panel). At the EP, the eigenmodes $\mathbf{E}_{1,2}^R$ coalesce into \mathbf{E}_0^R (upper-right panel). The Jordan vector (\mathbf{J}_0^R) was computed with a novel iterative method [41], and was used to verify Eq. (3).

Fig. 3b depicts the LDOS $_k$ for varying wavevectors k (where we omitted the subscript from k_x for brevity).

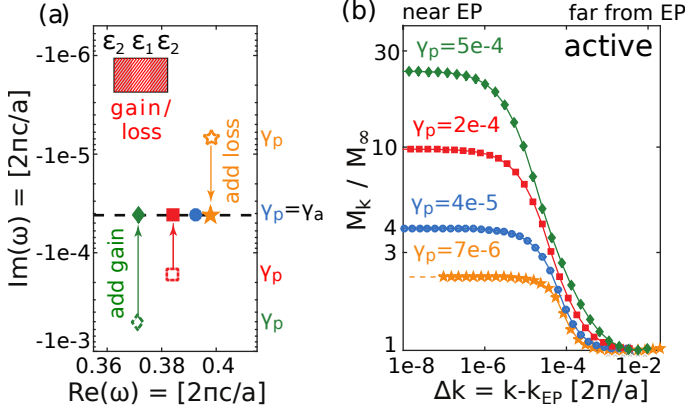


FIG. 4. **LDOS_k enhancement in active structures.** (a) Resonances with different passive loss rates γ_p (hollow symbols) and equal active loss rates γ_a (full symbols). Inset: Structure from Fig. 3a with gain/loss added to the waveguide. (b) Normalized LDOS_k peak (M_k/M_∞) vs. Δk , evaluated at \mathbf{r}_0 for the structures from (a), after adding gain/loss. The enhancement at the EP increases with the overall gain.

For $k \gg k_{\text{EP}}$ (denoted k_∞), the LDOS_k is a sum of two non-overlapping Lorentzians with peak value M_∞ . As k approaches the EP (e.g., at k_1 and k_2), the resonances begin to overlap and the LDOS_k peaks increase due to the growing PF (despite the unaltered decay rates, $\text{Im} \omega_n$). Most importantly, for k values near but not equal to k_{EP} , Eq. (1) is valid and it approaches Eq. (3) as $k \rightarrow k_{\text{EP}}$. Physically, this means that even if the structure does not have an exact EP, the LDOS_k peak is approximately M_{EP} . Computationally, this implies that as long as Maxwell's operator $A(k)$ is not exactly defective, one can use Eq. (1) to evaluate of the LDOS_k. The lower plot compares structures with varying quality factors. We change Q by modifying the permittivity contrast $\Delta\epsilon$; Radiation losses decrease with decreasing index contrast of the periodic modulation [42], with the limit of zero contrast corresponding to infinite Q . By plotting the normalized LDOS_k peak (M_k/M_∞) vs. deviation from the EP ($\Delta k \equiv k - k_{\text{EP}}$), we find that the enhancement at the EP is always approximately four-fold, regardless of Q . This follows from a sum rule which states that the spectrally integrated LDOS (and, therefore, also the LDOS_k) is a constant [43]. The ratio of peaks of two non-degenerate Lorentzians and a squared Lorentzian with the same γ is then equal to four, provided that they have the same spectrally integrated LDOS.

Even though the enhancement in passive systems is at most four-fold, significant PF enhancements can be achieved in active systems, i.e., by introducing gain. Fig. 4 compares four structures with different passive quality factors Q_p , with gain/loss added to the waveguide to achieve the same active quality factor Q_a . The empty (filled) markers in Fig. 4a are the EP resonances (ω_{EP}) in the complex plane before (after) adding gain/loss. As shown in Fig. 4b, the structure with the smallest passive

quality factor Q_p has the largest LDOS_k enhancement since it requires more gain in order to attain the same Q_a . (Larger enhancements are presented in the SM.)

We can interpret this result using TCMT. The uncoupled states in this case are the Γ -point modes, with resonant frequencies Ω_{EP} and $\Omega_{\text{EP}} - 2i\gamma_p$. The off-diagonal entries of the 2×2 matrix (H) which governs the dynamics are $\pm i v_g k$, where $v_g \equiv \frac{\partial \omega}{\partial k}|_{k=0}$ is the group velocity [19]. An EP occurs when $v_g k = \gamma_p$, with a complex frequency $\omega_{\text{EP}} = \Omega_{\text{EP}} - i\gamma_p$. When adding overall gain/loss, the EP moves vertically in the complex plane, becoming $\Omega_{\text{EP}} - i\gamma_a$, while the EP condition remains $k v_g = \gamma_p$. In analogy to Eq. (5), we find that the enhancement at the EP scales as $M_{\text{EP}} \propto \frac{\gamma_p}{\gamma_a^2} + \frac{1}{\gamma_a}$.

In both the plasmonic and the photonic examples, we found that the enhancement consisted of a quadratic term and a linear term (in Q), and we computed the coefficient of the quadratic term from TCMT. (In the plasmonic system, the coefficient was the coupling κ , while in the periodic example, the coefficient was γ_p .) More generally, we show in the SM that for arbitrary low-loss systems, the quadratic coefficient is bounded by

$$\kappa \leq \omega_{\text{EP}} \sqrt{\max |\text{Im} \epsilon|}. \quad (6)$$

This result provides an easy-to-evaluate upper bound on the maximal enhancements in complicated geometries. Note that in our plasmonic example, the quadratic coefficient is within 10% of the bound.

With the theory presented in this Letter, one can revisit some earlier proposals for giant PFs [44–46] and optimize the actual achievable enhancements in these systems. That could potentially be useful in applications requiring low-coherent light sources (e.g., optical coherence tomography [47]), or high-power high-spatial-resolution sources. Our theory could be extended to study the properties of lasers at EPs, which is important for modeling recent experimental work [20, 21, 48]. Since LDOS enhancement causes linewidth broadening above the lasing threshold [49], EPs may be useful for attaining coherence tunability, which is typically achieved with complicated circuitry [50]. Finally, our theory could be applied to study additional noise-driven processes (e.g., near-field heat transfer [51]) or EPs in other areas of physics (e.g., exciton-polariton [23] and mechanical systems [52]).

ACKNOWLEDGMENTS

This work was partially supported by the Army Research Office through the Institute for Soldier Nanotechnologies under Contract No. W911NF-13-D-0001. M.S. (reading and analysis of the manuscript) was supported by MIT S3TEC EFRC of the U.S. DOE under Grant No. DE-SC0001299. CWH was supported by the NSF grant No. DMR-1307632. AWR was supported by the NSF grant No. DMR-1454836. Finally, we would like to thank Aristeidis Karalis, Wonseok Shin, Nick Rivera, and David Liu for helpful discussions.

-
- [1] E. M. Purcell, "Spontaneous emission probabilities at radio frequencies," *Phys. Rev.* **69**, 681 (1946).
- [2] H. Yokoyama and K. Ujihara, *Spontaneous emission and laser oscillation in microcavities*, Vol. 10 (CRC press, 1995).
- [3] S. V. Gaponenko, *Introduction to nanophotonics* (Cambridge University Press, 2010).
- [4] W. J. Firth and A. M. Yao, "Giant excess noise and transient gain in misaligned laser cavities," *Phys. Rev. Lett.* **95**, 073903 (2005).
- [5] M. V. Berry, "Mode degeneracies and the petermann excess-noise factor for unstable lasers," *J. of mod. opt.* **50**, 63–81 (2003).
- [6] S-Y Lee, J-W Ryu, J-B Shim, S-B Lee, S. W. Kim, and K. An, "Divergent petermann factor of interacting resonances in a stadium-shaped microcavity," *Phys. Rev. A* **78**, 015805 (2008).
- [7] K. Petermann, "Calculated spontaneous emission factor for double-heterostructure injection lasers with gain-induced waveguiding," *IEEE J. Quant. Elect.* **15**, 566–570 (1979).
- [8] M. A. Van Eijkelenborg, Å. M. Lindberg, M. S. Thijssen, and J. P. Woerdman, "Resonance of quantum noise in an unstable cavity laser," *Phys. Rev. Lett.* **77**, 4314 (1996).
- [9] A. M. Van der Lee, N. J. Van Druten, A. L. Mieremet, M. A. Van Eijkelenborg, Å. M. Lindberg, J. P. M. P. Van Exter, and Woerdman, "Excess quantum noise due to nonorthogonal polarization modes," *Phys. Rev. Lett.* **79**, 4357 (1997).
- [10] A. E. Siegman, "Excess spontaneous emission in non-hermitian optical systems. i. laser amplifiers," *Phys. Rev. A* **39**, 1253–1263 (1989).
- [11] A. E. Siegman, "Excess spontaneous emission in non-hermitian optical systems. ii. laser oscillators," *Phys. Rev. A* **39**, 1264–1268 (1989).
- [12] N. Moiseyev, *Non-Hermitian Quantum Mechanics* (Cambridge University Press, 2011) pp. 174–183.
- [13] A. P. Seyranian and A. A. Mailybaev, *Multiparameter Stability Theory With Mechanical Applications* (World Scientific Publishing, 2003).
- [14] W. D. Heiss, "The physics of exceptional points," *J. Phys. A - Math. Theo.* **45**, 444016 (2012).
- [15] L. N. Trefethen and M. Embree, *Spectra and pseudospectra: the behavior of nonnormal matrices and operators* (Princeton University Press, 2005).
- [16] S. H. Weintraub, "Jordan canonical form: application to differential equations," *Synthesis Lectures on Mathematics and Statistics* **1**, 1–85 (2008).
- [17] G. Yoo, H-S Sim, and H. Schomerus, "Quantum noise and mode nonorthogonality in non-hermitian pt-symmetric optical resonators," *Phys. Rev. A* **84**, 063833 (2011).
- [18] A. M. van den Brink, K. Young, and M. H. Yung, "Eigenvector expansion and petermann factor for ohmically damped oscillators," *J. PhysA: Math. Gen.* **39**, 3725 (2006).
- [19] B. Zhen, C. W. Hsu, Y. Igarashi, L. Lu, I. Kaminer, A. Pick, S-L Chua, J. D. Joannopoulos, and M. Soljačić, "Spawning rings of exceptional points out of dirac cones," *Nature* **525**, 354–358 (2015).
- [20] H. Hodaei, M-A Miri, M. Heinrich, D. N. Christodoulides, and M. Khajavikhan, "Parity-time-symmetric microring lasers," *Science* **346**, 975–978 (2014).
- [21] L. Feng, Z. J. Wong, R-M Ma, Y. Wang, and X. Zhang, "Single-mode laser by parity-time symmetry breaking," *Science* **346**, 972–975 (2014).
- [22] L. Feng, Y-L Xu, W. S. Fegadolli, M-H Lu, J. EB Oliveira, V. R. Almeida, Y-F Chen, and A. Scherer, "Experimental demonstration of a unidirectional reflectionless parity-time metamaterial at optical frequencies," *Nature materials* **12**, 108–113 (2013).
- [23] T. Gao, E. Estrecho, K. Y. Bliokh, T. C. H. Liew, M. D. Fraser, S. Brodbeck, M. Kamp, C. Schneider, S. Hofling, Y. Yamamoto, *et al.*, "Observation of non-hermitian degeneracies in a chaotic exciton-polariton billiard," *Nature* **526**, 554–558 (2015).
- [24] F. Wijnands, J. B. Pendry, F. J. Garcia-Vidal, and P. J. Roberts P. M. Bell, and L. Martin Moreno, "Green's functions for maxwell's equations: application to spontaneous emission," *Opt. and Quant. Elect.* **29**, 199–216 (1997).
- [25] Y. Xu, R. K. Lee, and A. Yariv, "Quantum analysis and the classical analysis of spontaneous emission in a microcavity," *Phys. Rev. A* **61**, 033807 (2000).
- [26] K. Sakoda, *Optical properties of photonic crystals*, Vol. 80 (Springer Science & Business Media, 2004).
- [27] A. Lagendijk and B. A. Van Tiggelen, "Resonant multiple scattering of light," *Phys. Rep.* **270**, 143–215 (1996).
- [28] A. Taflove, A. Oskooi, and S. G. Johnson, *Advances in FDTD Computational Electrodynamics: Photonics and Nanotechnology* (Artech House, 2013) p. 76.
- [29] G. B. Arfken and H. J. Weber, *Mathematical Methods for Physicists* (Elsevier Academic Press, 2006) pp. 184–185.
- [30] J. D. Joannopoulos, S. G. Johnson, J. N. Winn, and R. D. Meade, *Photonic crystals: molding the flow of light* (Princeton university press, 2011).
- [31] P. M. Morse and H. Feshbach, "Methods of theoretical physics," *International Series in Pure and Applied Physics*, New York: McGraw-Hill, 1953 **1** (1953).
- [32] A. E. Siegman, "Lasers university science books," Mill Valley, CA **37** (1986).
- [33] H. E. Türeci, A. D. Stone, and B. Collier, "Self-consistent multimode lasing theory for complex or random lasing media," *Phys. Rev. A* **74**, 043822 (2006).
- [34] G. W. Hanson, A. I. Nosich, and E. M. Kartchevski, "Green's function expansions in dyadic root functions for shielded layered waveguides," *PIER* **39**, 61–91 (2003).
- [35] E. Hernández, A. Jàuregui, and A. Mondragón, "Jordan blocks and gamow-jordan eigenfunctions associated with a degeneracy of unbound states," *Phys. Rev. A* **67**, 022721 (2003).
- [36] W. D. Heiss, "Green's functions at exceptional points," *Int. J. Theo. Phys.*, 1–6 (2015).
- [37] H. L. A. Christ and Hartnagel, "Three-dimensional finite-difference method for the analysis of microwave-device embedding," *IEEE Transactions on Microwave Theory Techniques* **35**, 688–696 (1987).
- [38] W. P. Huang, "Coupled-mode theory for optical waveguides: an overview," *JOSA A* **11**, 963–983 (1994).
- [39] N. W. Ashcroft and N. D. Mermin, "Solid state phys," Saunders, Philadelphia **293** (1976).

- [40] R. C. McPhedran, L. C. Botten, J. McOrist, A. A. Asatryan, C. M. de Sterke, and N. A. Nicorovici, “Density of states functions for photonic crystals,” *Physical Review E* **69**, 016609 (2004).
- [41] F. Hernandez et al. In preparation.
- [42] H. Benisty, D. Labilloy, C. Weisbuch, C. J. M. Smith, T. F. Krauss, D. Cassagne, A. Beraud, and C. Jouanin, “Radiation losses of waveguide-based two-dimensional photonic crystals: Positive role of the substrate,” *Applied Physics Letters* **76**, 532–534 (2000).
- [43] S. M. Barnett and R. Loudon, “Sum rule for modified spontaneous emission rates,” *Phys. Rev. Lett.* **77**, 2444 (1996).
- [44] S. Longhi, “Enhanced excess noise in laser cavities with tilted mirrors,” *Opt. lett.* **25**, 811–813 (2000).
- [45] G. D’Alessandro and C. B. Laforet, “Giant noise amplification in synchronously pumped optical parametric oscillators,” *Opt. Lett.* **34**, 614–616 (2009).
- [46] G. D’Alessandro and F. Papoff, “Giant subthreshold amplification in synchronously pumped optical parametric oscillators,” *Phys. Rev. A* **80**, 023804 (2009).
- [47] J. G. Fujimoto, C. Pitris, S. A. Boppart, and M. E. Brezinski, “Optical coherence tomography: an emerging technology for biomedical imaging and optical biopsy,” *Neoplasia* **2**, 9–25 (2000).
- [48] M. Brandstetter, M. Liertzer, C. Deutsch, P. Klang, J. Schöberl, H. E. Türeci, G. Strasser, K. Unterrainer, and S. Rotter, “Reversing the pump dependence of a laser at an exceptional point,” *Nat. comm.* **5** (2014).
- [49] A. Pick, A. Cerjan, D. Liu, A. W. Rodriguez, A. D. Stone, Y. D. Chong, and S. G. Johnson, “*Ab initio* multimode linewidth theory for arbitrary inhomogeneous laser cavities,” *Phys. Rev. A* **91**, 063806 (2015).
- [50] J. D. McKinney, M. A. Webster, K. J. Webb, and A. M. Weiner, “Characterization and imaging in optically scattering media by use of laser speckle and a variable-coherence source,” *Optics Letters* **25**, 4–6 (2000).
- [51] C. Khandekar, W. Jin, O. D. Miller, A. Pick, and A. W. Rodriguez, “Giant frequency-selective near-field heat transfer in *pt*-symmetric structures,” arxiv: 1511.04492.
- [52] L. Jiang H. Xu, D. Mason and J. G. E. Harris, “Topological energy transfer in an optomechanical system with exceptional points,” arxiv: 1602.06881.
- [53] A. P. Seyranian and A. A. Mailybaev, *Multiparameter stability theory with mechanical applications*, Vol. 13 (World Scientific, 2003).
- [54] K. Okamoto, *Fundamentals of optical waveguides* (Academic press, 2010) pp. 159–166.
- [55] P. N. Butcher and D. Cotter, *The elements of nonlinear optics*, Vol. 9 (Cambridge University Press, 1991) p. 216.

SUPPLEMENTARY INFORMATION

I. PERTURBATION THEORY NEAR THE EP

In this section, we derive an eigenvalue expansion formula for the Green's function, which is valid at the EP [Eq. (3) in the text], by taking three main steps: First, we express the eigenvalues $\lambda_{\pm} \equiv \omega_{\pm}^2$ and eigenmodes $\mathbf{E}_{\pm}^{R,L}$ near the EP in terms of the degenerate quantities $\mathbf{E}_0^{R,L}$, $\mathbf{J}_0^{R,L}$ and λ_{EP} . Then, we substitute these expressions into the expansion formula for non-degenerate poles Eq. (S13) and last, we take the limit of approaching the EP.

The non-degenerate eigenvectors and eigenvalues near the EP satisfy the generalized eigenvalue problem

$$A(p)\mathbf{E}_{\pm}^R = \lambda_{\pm}\mathbf{E}_{\pm}^R, \quad (\text{S1})$$

where p represents the deviation from the EP. For example, in the plasmonic example (Fig. 1a), p is a dimensionless deviation of the gain/loss parameter from the critical value, $p \equiv \frac{\eta - \eta_{\text{EP}}}{\Omega_{\text{EP}}}$, and $A(p) = \varepsilon(p)^{-1} \nabla \times \nabla \times$. Near the EP (i.e., for $|p| \ll 1$), we can expand $A(p) = A_0 + A_1 p + \mathcal{O}(p^2)$, where $A_0 \equiv \frac{1}{\varepsilon(0)} \nabla \times \nabla \times$ and $A_1 \equiv -\frac{\Theta}{\varepsilon(0)^2} \nabla \times \nabla \times$ (Θ is the step function defined as 1 inside the gain/loss region and 0 elsewhere).

For convenience, we discretize Maxwell's equations in this section (e.g., via FDFD), but the results we derive apply to the continuous equations as well (by taking the limit of infinite number of grid points). At the EP, the right eigenvector and Jordan vector satisfy the chain relations

$$A_0 \mathbf{E}_0^R = \lambda_{\text{EP}} \mathbf{E}_0^R, \quad (\text{S2})$$

$$A_0 \mathbf{J}_0^R = \lambda_{\text{EP}} \mathbf{J}_0^R + \mathbf{E}_0^R \quad (\text{S3})$$

and, similarly, the left eigenvectors satisfy

$$A_0^T \mathbf{E}_0^L = \lambda_{\text{EP}} \mathbf{E}_0^L, \quad (\text{S4})$$

$$A_0^T \mathbf{J}_0^L = \lambda_{\text{EP}} \mathbf{J}_0^L + \mathbf{E}_0^L. \quad (\text{S5})$$

We can choose the normalization conditions $(E_0^L, J_0^R) = 1$ and $(J_0^L, J_0^R) = 0$, where round brackets denote the unconjugated inner product $(a, b) \equiv a^T b$.

Consistent perturbative expressions near the EP can be obtained by expanding \mathbf{E}_{\pm} and λ_{\pm} in an alternating Puiseux series [53]

$$\lambda_{\pm} = \lambda_{\text{EP}} \pm p^{\frac{1}{2}} \lambda_1 + p \lambda_2 \pm p^{\frac{3}{2}} \lambda_3 + \dots \quad (\text{S6})$$

$$\mathbf{E}_{\pm}^R = \mathbf{E}_0^R \pm p^{\frac{1}{2}} \mathbf{E}_1^R + p \mathbf{E}_2^R \pm p^{\frac{3}{2}} \mathbf{E}_3^R + \dots \quad (\text{S7})$$

Substituting the above expansions for λ_{\pm} , $\mathbf{E}_{\pm}^{R,L}$, and A into Eq. (S1), and requiring the addition normalization condition $(J_0^L, E_{\pm}^R) = 1$ [which implies $(J_0^L, E_n^R) = 0$ for

all $n \geq 1$], one obtains [53]

$$\lambda_1 = \sqrt{(E_0^L, A_1, E_0^R)}, \quad (\text{S8})$$

$$\lambda_2 = \frac{(E_0^L, A_1, J_0^R) + (J_0^L, A_1, E_0^R)}{2} \quad (\text{S9})$$

$$\mathbf{E}_1^R = \lambda_1 \mathbf{J}_0^R \quad (\text{S10})$$

$$\mathbf{E}_2^R = \lambda_2 \mathbf{J}_0^R + (G_1^R)^{-1} (\lambda_1^2 \mathbf{J}_0^R - A_1 \mathbf{E}_0^R) \quad (\text{S11})$$

$$G_1^R = A_0 - \lambda_{\text{EP}} I - \lambda_{\text{EP}} \mathbf{E}_0^R (\mathbf{J}_0^L)^T, \quad (\text{S12})$$

where we have introduced the notation $(\psi^L, A, \psi^R) \equiv (\psi^L)^T A \psi^R$. Similar expressions are obtained for the left vectors \mathbf{E}_1^L and \mathbf{E}_2^L .

Next, we substitute Eqs. (S8-S12) into the Green's function expansion formula for non-degenerate modes [29]

$$G(\omega) \approx \frac{\mathbf{E}_+^R (\mathbf{E}_+^L)^T}{(\omega^2 - \omega_+^2) (E_+^L, E_+^R)} + \frac{\mathbf{E}_-^R (\mathbf{E}_-^L)^T}{(\omega^2 - \omega_-^2) (E_-^L, E_-^R)}. \quad (\text{S13})$$

The denominators vanish upon approaching the EP [since $(E_{\pm}, E_{\pm}) = \pm 2 p^{\frac{1}{2}} \lambda_1 + \mathcal{O}(p)$, as can be seen from Eqs. (S7, S10)]. Most importantly, the opposite signs of the denominators in Eq. (S13) lead to cancellation of the divergences and to the finite LDOS. More explicitly, in the limit of $p \rightarrow 0$, the following relation holds:

$$\lim_{p \rightarrow 0} \left[\sum_{i=\pm} \frac{\mathbf{E}_i^R (\mathbf{E}_i^L)^T}{(\omega^2 - \omega_i^2) (E_i^L, E_i^R)} \right] = \frac{1}{(\omega^2 - \omega_{\text{EP}}^2)^2} \frac{\mathbf{E}_0^R (\mathbf{E}_0^L)^T}{(E_0^L, J_0^R)} + \frac{1}{\omega^2 - \omega_{\text{EP}}^2} \frac{\mathbf{E}_0^R (J_0^L)^T + J_0^R (\mathbf{E}_0^L)^T}{(E_0^L, J_0^R)}. \quad (\text{S14})$$

Using this result we obtain

$$G_{\text{EP}} = \frac{1}{(\omega^2 - \omega_{\text{EP}}^2)^2} \frac{\mathbf{E}_0^R (\mathbf{E}_0^L)^T}{(E_0^L, J_0^R)} + \frac{1}{\omega^2 - \omega_{\text{EP}}^2} \frac{\mathbf{E}_0^R (J_0^L)^T + J_0^R (\mathbf{E}_0^L)^T}{(E_0^L, J_0^R)}, \quad (\text{S15})$$

thus completing the proof of Eq. (3).

II. DERIVATION OF TCMT [EQ. (4)]

In this section, we review the derivation of TCMT [38, 54]. We derive equations governing the field evolution of two coupled rods (Fig. 1a) in terms of the modes of a system of two uncoupled rods [i.e., when the rod-rod separation (t_1) is infinite]. The field of the coupled system satisfies Maxwell's wave equation:

$$\nabla \times \nabla \times \mathcal{E} = \varepsilon \partial_t^2 \mathcal{E}. \quad (\text{S16})$$

Denoting by ε_p the permittivity of a system which contains a single rod ($p = 1, 2$), the modes of the non-interacting system satisfy

$$\nabla \times \nabla \times \mathbf{E}_p = \varepsilon_p \omega_p^2 \mathbf{E}_p, \quad (\text{S17})$$

where $\mathcal{E}_p(x, t) = \mathbf{E}_p(x) e^{-i\omega_p t}$. In the weak-coupling regime (i.e., when the rod-rod separation is large enough

so that the frequency splitting induced by their interaction is much smaller than $\text{Re } \omega_p$, the field of the interacting system \mathcal{E} can be written approximately as a weighed sum of the non-interacting modes:

$$\mathcal{E}(x, t) \approx a_1(t) \mathbf{E}_1(x) e^{-i\omega_1 t} + a_2(t) \mathbf{E}_2(x) e^{-i\omega_2 t}. \quad (\text{S18})$$

The second order time derivative of the field is

$$\partial_t^2 \mathcal{E} \approx - \sum_p (2i\omega_p \dot{a}_p + \omega_p^2 a_p) \mathbf{E}_p e^{-i\omega_p t}, \quad (\text{S19})$$

where we have used the slowly varying amplitude approximation (SVEA) [55] to omit \ddot{a} . Substituting Eqs. (S17-S19) into Maxwell's equation Eq. (S16), one obtains

$$\sum_p [2i\omega_p \dot{a}_p \varepsilon + \omega_p^2 a_p (\varepsilon - \varepsilon_p)] \mathbf{E}_p e^{-i\omega_p t} = 0 \quad (\text{S20})$$

In order to derive equations of motion for a_j , we multiply Eq. (S20) by \mathbf{E}_j and integrate over space. We use the bi-orthogonality relation $\int \mathbf{E}_1 \mathbf{E}_2 = 0$ and the normalization condition $\int \mathbf{E}_j^2 = 1$, and we assume, for simplicity, that the uncoupled resonances are degenerate $\omega_1 = \omega_2 = \omega_{\text{EP}} \equiv \Omega_{\text{EP}} - i\gamma$. Note that terms $\propto \int \Delta \varepsilon_j \mathbf{E}_j^2$ can be omitted since $\Delta \varepsilon_j \equiv \varepsilon - \varepsilon_j$ is nonzero only inside resonator $k \neq j$ and the field \mathbf{E}_j is small inside resonator $k \neq j$. Consequently, we obtain

$$\begin{aligned} \dot{a}_1 &= i\kappa_1 a_2 \\ \dot{a}_2 &= i\kappa_2 a_1 \end{aligned} \quad (\text{S21})$$

where $\kappa_j \equiv \frac{\omega_j}{2} \int \Delta \varepsilon_k \mathbf{E}_j \mathbf{E}_k$. Since the geometry we consider here is nearly symmetric with respect to the $y = 0$ axis (Fig. 1a), we can assume $\kappa_1 \approx \kappa_2$. Introducing $\tilde{a}_j \equiv a_j e^{-i\omega_j t}$ and including a frequency shift which is induced by adding gain/loss to the coatings, we obtain the TCMT equations Eq. (4)

$$\begin{aligned} \dot{\tilde{a}}_1 &= i(\omega_{\text{EP}} - i\eta) \tilde{a}_1 + i\kappa \tilde{a}_2 \\ \dot{\tilde{a}}_2 &= i(\omega_{\text{EP}} + i\eta) \tilde{a}_2 + i\kappa \tilde{a}_1 \end{aligned} \quad (\text{S22})$$

In the following section, we relate the Green's function of Maxwell's operator at the EP (A_0) to the the 2×2 restriction of A_0 onto the subspace spanned by the basis vectors \mathbf{E}_1 and \mathbf{E}_2 (\bar{A}_0). Using the same notation as above, one can verify that the diagonal terms of \bar{A}_0 are $\int \mathbf{E}_j \frac{1}{\varepsilon} \nabla \times \nabla \times \mathbf{E}_j \approx \int \mathbf{E}_j \frac{1}{\varepsilon_j} \nabla \times \nabla \times \mathbf{E}_j = \omega_j^2$, whereas the off-diagonal terms are $\int \mathbf{E}_k \frac{1}{\varepsilon} \nabla \times \nabla \times \mathbf{E}_j \approx -\omega_j^2 \int \frac{\Delta \varepsilon_j}{\varepsilon^2} \mathbf{E}_j \mathbf{E}_k$. For convenience, one can discretize space (e.g., by FDFD) and recast Maxwell's operator A_0 in matrix form. Denoting by X the matrix whose columns are \mathbf{E}_1 and \mathbf{E}_2 , one can show that in the limit of $\gamma \ll \Omega_{\text{EP}}$,

$$\bar{A}_0 = X^T A_0 X = \begin{pmatrix} (\omega_{\text{EP}} - i\eta)^2 & 2\Omega_{\text{EP}} \kappa \\ 2\Omega_{\text{EP}} \kappa & (\omega_{\text{EP}} + i\eta)^2 \end{pmatrix} \quad (\text{S23})$$

III. TCMT APPROXIMATION FOR THE LDOS

In the main text, we use an approximate expression for the LDOS which we derive from TCMT. In this section, we provide a justification for this approach. As in the previous section, we discretize space (e.g., by FDFD) and recast Maxwell's operator A_0 in matrix form. We begin by relating the Green's function at the EP (G_{EP}) to the resolvent of \bar{A}_0 :

$$G_{\text{EP}}(\mathbf{r}, \mathbf{r}', \omega) \equiv (A_0 - \omega^2 \mathbb{1})^{-1} \approx X (\bar{A}_0 - \omega^2 \mathbb{1})^{-1} X^T, \quad (\text{S24})$$

which is valid when G_{EP} is dominated by the two coalescing resonances. The LDOS, as measured by a dipole source at position i , is given by [28]

$$\begin{aligned} \text{LDOS}(\mathbf{r}_i, \omega) &= -\text{Im} [e_i^T G(\mathbf{r}, \mathbf{r}', \omega) e_i] \approx \\ &= -\text{Im} [(e_i^T X) (\bar{A}_0 - \omega^2 \mathbb{1})^{-1} (X^T e_i)], \end{aligned} \quad (\text{S25})$$

where e_i is a unit vector (with 1 in the i 'th entry). The diagonal entries of the 2×2 resolvent operator are

$$\bar{R} \equiv (\bar{A}_0 - \omega^2 \mathbb{1})_{[i,i]}^{-1} = \frac{1}{\omega^2 - \omega_{\text{EP}}^2} + (-1)^{i-1} \frac{2\Omega_{\text{EP}} \kappa}{[\omega^2 - \omega_{\text{EP}}^2]^2}. \quad (\text{S26})$$

Eqs. (S25, S26) can be used to interpret the FDFD results. When the point \mathbf{r}_i is a node of \mathbf{E}_2 [i.e., $\mathbf{E}_2(\mathbf{r}_i) = 0$], the LDOS is proportional to the first diagonal entry of \bar{R} :

$$\text{LDOS}_k(\mathbf{r}_i, \omega) \approx -\text{Im} [\mathbf{E}_1^R(\mathbf{r}_i)^2 \left(\frac{1}{\omega^2 - \omega_{\text{EP}}^2} + \frac{2\Omega_{\text{EP}} \kappa}{[\omega^2 - \omega_{\text{EP}}^2]^2} \right)]. \quad (\text{S27})$$

(This is the case, for example, at r_A in Fig. 1a, where \mathbf{E}_2 is concentrated in the lower resonator.) This expression can be further simplified in the regime of $\gamma \ll \Omega_{\text{EP}}$ and when the modes \mathbf{E}_1 and \mathbf{E}_2 are almost real (i.e., $\text{Im}[\mathbf{E}] \approx 0$). After some more algebra, we obtain

$$\begin{aligned} \text{LDOS}_k(\mathbf{r}_i, \omega) &\approx \\ \frac{\mathbf{E}_1^R(\mathbf{r}_i)^2}{2\Omega_{\text{EP}}} &\left[\frac{\gamma}{(\omega - \Omega_{\text{EP}})^2 + \gamma^2} + \frac{\kappa [\gamma^2 - (\omega - \Omega_{\text{EP}})^2]}{[\gamma^2 - (\omega - \Omega_{\text{EP}})^2]^2 + [2\gamma(\omega - \Omega_{\text{EP}})]^2} \right] \end{aligned} \quad (\text{S28})$$

The full-width half maximum (FWHM) is denoted by Γ , where $\Gamma/2$ is the frequency at which the LDOS drops to half of its maximal value [i.e., $\text{LDOS}_k(\mathbf{r}_i, \Gamma/2) = \frac{1}{2} \max_{\omega} \{\text{LDOS}_k(\mathbf{r}_i, \omega)\}$]. It follows from Eq. (S28) that the FWHM at the EP is

$$\Gamma = 2\gamma \sqrt{\frac{\sqrt{\gamma^2 + 2\gamma\kappa + 5\kappa^2} - 2\kappa}{\gamma + \kappa}} \quad (\text{S29})$$

with the limit of $2\gamma\sqrt{\sqrt{5} - 2}$ when $\kappa \rightarrow \infty$.

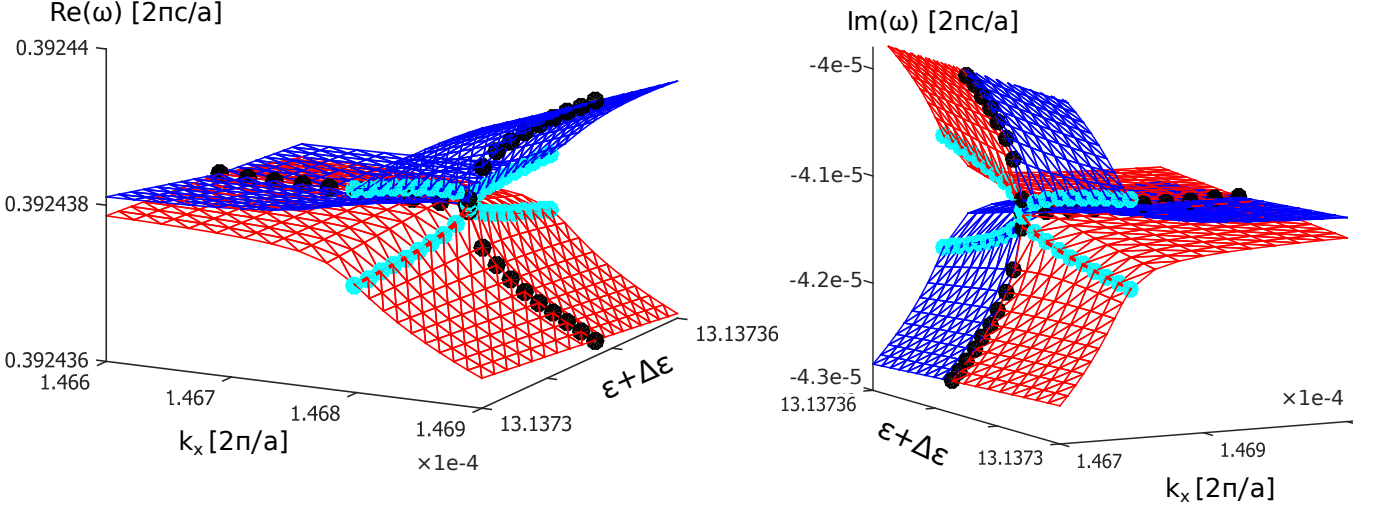


FIG. S1. **Eigenvalue surfaces (blue and red sheets) of periodic waveguides.** (a) Real and (b) imaginary parts of the eigenvalues of $A(k) \equiv \varepsilon^{-1}(\nabla + i\mathbf{k}) \times (\nabla + i\mathbf{k}) \times$ as a function of the wavevector k_x and the permittivity contrast $\Delta\varepsilon \equiv \varepsilon_2 - \varepsilon_1$, for the geometry from Fig. 3a. The EP ($\omega_{\text{EP}} = 0.3924377 - 0.00004119303i$) occurs at $k_{\text{EP}}a/2\pi \approx 1.468 \times 10^{-4}$ and $\Delta\varepsilon_{\text{EP}} \approx 1.137$. Cyan: Eigenvalues for fixed $k_x = k_{\text{EP}}$ and varying $\Delta\varepsilon$. Black: Eigenvalues for fixed $\Delta\varepsilon = \Delta\varepsilon_{\text{EP}}$ and varying k_x .

IV. UPPER BOUND FOR EP ENHANCEMENT

Let us first define an effective mode amplitude $\langle \psi, \psi \rangle \equiv \int_C dx |\psi|^2$, where C denotes a finite region containing the geometry (e.g., the last scattering surface). In order to obtain an upper bound on the LDOS enhancement at the EP, we need to estimate the quantities $\langle E_0^R, E_0^R \rangle / \langle J_0^R, J_0^R \rangle$ and $\langle E_0^L, E_0^L \rangle / \langle J_0^L, J_0^L \rangle$, which determine the relative magnitude of the two terms in Eq. (3). Let us decompose the complex-symmetric Maxwell's operator into: $A = A' + iA''$, where $A' \equiv \frac{A+A^*}{2}$ and $A'' \equiv \frac{A-A^*}{2i}$, and the asterisk denotes complex conjugation. In many cases of interest, one can assume $\|A''\| \ll \|A'\|$ (under an appropriate matrix norm). In such cases, one can use perturbation theory (SM I) to expand the eigenmodes \mathbf{E}_\pm^R and eigenvalues ω_\pm of A' in terms \mathbf{E}_0 , \mathbf{J}_0 and λ_{EP} . It follows from Eqs. (S7,S10) that

$$\mathbf{E}_0^R \approx (\mathbf{E}_+^R + \mathbf{E}_-^R)/2 \quad (\text{S30})$$

$$\mathbf{J}_0^R \approx (\mathbf{E}_+^R - \mathbf{E}_-^R)/(2\lambda_1 p^{\frac{1}{2}}). \quad (\text{S31})$$

Since A' is a real Hermitian operator, it has real and orthogonal eigenvectors \mathbf{E}_\pm . Using Eqs. (S30,S31) and assuming $\langle E_+, E_+ \rangle \approx \langle E_-, E_- \rangle$ and $\langle E_-, E_+ \rangle = 0$, one obtains

$$\begin{aligned} \langle E_0^R, E_0^R \rangle &\approx \langle E_+, E_+ \rangle / 2 \\ \langle J_0^R, J_0^R \rangle &\approx \langle E_+, E_+ \rangle / 2|\lambda_1|^2 p. \end{aligned} \quad (\text{S32})$$

Using Eq. (S8), we find that

$$\frac{\langle E_0^R, E_0^R \rangle}{\langle J_0^R, J_0^R \rangle} \approx |\lambda_1|^2 p \approx \left| \frac{(E_0^L, A'', E_0^R)}{(J_0^L, E_0^R)} \right|. \quad (\text{S33})$$

A similar analysis leads to an equivalent expression for the left eigenvectors. Next, recall the definition of $A \equiv \frac{1}{\varepsilon} \nabla \times \nabla \times$. In the limit of $\|\text{Im} \varepsilon / \varepsilon\| \ll 1$, we can approximate $A'' \approx -\frac{\text{Im} \varepsilon}{\varepsilon^2} \nabla \times \nabla \times$ and, consequently

$$\begin{aligned} |(E_0^L, A'', E_0^R)| &\approx \omega_{\text{EP}}^2 \left| \int \mathbf{E}_0^L (\text{Im} \varepsilon / \varepsilon) \mathbf{E}_0^R \right| = \\ \omega_{\text{EP}}^2 \left| \int \text{Im} \varepsilon \mathbf{E}_0^{R2} \right| &\approx \omega_{\text{EP}}^2 \left| \int \text{Im} \varepsilon |\mathbf{E}_0^R|^2 \right| \leq \omega_{\text{EP}}^2 \max |\text{Im} \varepsilon|, \end{aligned} \quad (\text{S34})$$

where, in going from the first to the second line, we used the relation $\mathbf{E}_0^R = \varepsilon^{-1} \mathbf{E}_0^L$ (which holds for Maxwell's eigenvalue problem) and, in the following approximations, we used the property $\mathbf{E}_0^2 \approx |\mathbf{E}_0|^2$ (valid for of low-loss systems) and the normalization condition $\int |\mathbf{E}_0|^2 = 1$.

V. FORCING AN EP IN PERIODIC WAVEGUIDES

We find EPs in the FDFD matrix discretization of Maxwell's equations by minimizing the distance between eigenvalues while searching the 2D parameter space spanned by the wavevector k_x and the permittivity contrast $\Delta\varepsilon$. The results of this numerical procedure are shown in Fig. S1.

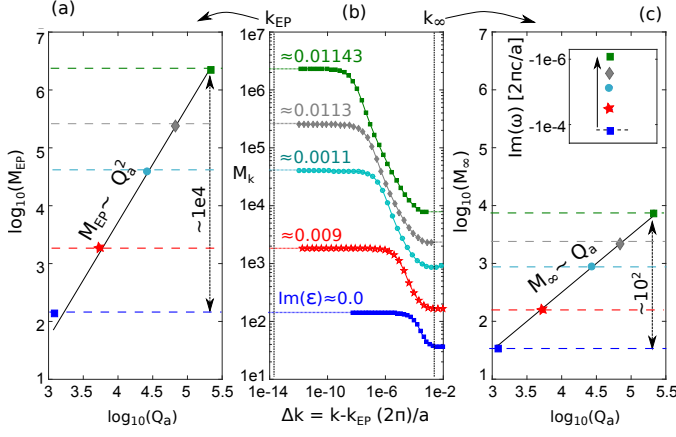


FIG. S2. **LDOS enhancement in active periodic waveguides.** Middle: LDOS peak vs. Δk , evaluated for the structure from Fig. 3 for increasing amounts of gain in the waveguide. Left: $\log_{10}(M_{EP})$ vs. $\log_{10}(Q_a)$ for the data from the middle panel near k_{EP} , showing quadratic scaling with Q_a . Right: $\log_{10}(M_{\infty})$ vs. $\log_{10}(Q_a)$ for the data from the middle panel at k_{∞} , showing linear scaling with Q_a . Inset: Eigenvalues move vertically in the complex plane upon adding gain.

VI. LDOS_k ENHANCEMENT WITH GAIN

In this section, we consider a periodic waveguide (as shown in Fig. 3), with periodic index modulation along \hat{x} and outgoing boundary conditions in the transverse y -direction. The design parameters in this section are $\varepsilon_1 = 12$, $\varepsilon_2 \approx 14.43$, $a = 1$, and $d = 0.4807$. Fig. S2b depicts the LDOS_k peak value vs. deviation from the EP ($\Delta k \equiv k - k_{EP}$) when adding varying amounts of gain to the waveguide (i.e., here we fix Q_p while increasing Q_a). The LDOS is evaluated at r_0 (Fig. 3a) using FDFD. We achieve enhancements of ≈ 400 . (Higher values can easily be obtained; the enhancement is essentially not bounded in this computational model. However, in reality, it is bounded by quantum noise near threshold[49].) We find that the LDOS peak scales quadratically with Q_a near the EP (as shown in Fig. S2a) and linearly with Q_a away from the EP (as shown in Fig. S2c). When the LDOS is evaluated near the center of the computational cell (i.e., at $x \approx 0$), the lineshape changes dramatically, and it actually has a minimum at the resonance frequency and two side peaks, whose amplitude scales as Q_a^2 (not shown).